



# Marine diatoms in ice cores from the Antarctic Peninsula and Ellsworth Land, Antarctica – species diversity and regional variability

Dieter R. Tetzner<sup>1,2</sup>, Elizabeth R. Thomas<sup>1</sup>, Claire Allen<sup>1</sup>

5 <sup>1</sup>British Antarctic Survey, Ice Dynamics and Paleoclimate, Cambridge, CB3 0ET, UK

<sup>2</sup>Department of Earth Sciences, University of Cambridge, Cambridge, CB2 3EQ, UK

*Correspondence to:* Dieter R. Tetzner (dietet95@bas.ac.uk)

**Abstract.** The presence of marine microfossils (diatoms) in glacier ice and ice cores has been documented from numerous sites in Antarctica, Greenland, as well as from sites in the Andes and the Altai mountains, and attributed to entrainment and transport by winds. However, their presence and diversity in snow and ice, especially in polar regions, is not well documented and still poorly understood. Here we present the first data to resolve the regional and temporal distribution of diatoms in ice cores, spanning a 20 year period across four sites in the southern Antarctic Peninsula and Ellsworth Land, Antarctica. We assess the regional variability in diatom composition and abundance at annual and sub-annual resolution across all four sites. These data corroborate the dominance of contemporary marine diatoms in Antarctic Peninsula ice cores, reveal that the timing and amount of diatoms deposited vary between low and high elevation sites and support existing evidence that marine diatoms have the potential to yield a novel wind paleoenvironmental proxy for ice cores in the southern Antarctic Peninsula and Ellsworth Land.

## 1 Introduction

Diatoms are unicellular algae with siliceous cell walls that inhabit aquatic environments throughout the world (Smol and Stoermer, 2010). They are especially abundant and diverse in the Southern Ocean (SO) (Zielinski and Gersonde, 1997; Armand et al., 2005; Crosta et al., 2005; Alvain et al., 2008). Diatoms are particularly sensitive to oceanographic conditions and responsive to environmental changes. These characteristics make them valuable as proxies for paleoenvironmental and palaeoceanographic reconstructions (Smol and Stoermer, 2010). Despite their aquatic habitats, several studies support they can be airborne (Lichti-Federovich, 1984; Gayley et al., 1989; Chalmers et al., 1996; McKay et al., 2008; Wang et al., 2008; Harper and McKay, 2010; Spaulding et al., 2010; Hausmann et al., 2011; Budgeon et al., 2012; Papina et al., 2013; Fritz et al., 2015). Diatoms can be effectively lifted from the sea-surface microlayer into the atmosphere by wind-induced bubble-bursting and wave-breaking processes (Cipriano and Blanchard, 1981; Farmer et al., 1993). Once in the atmosphere, they can be transported by winds over long distances (Gayley et al., 1989; McKay et al., 2008; Harper and McKay, 2010). In Polar



Regions, airborne diatoms can be deposited over ice sheets (Budgeon et al., 2012; Allen et al., 2020) and then buried under  
30 subsequent snowfall events to finally become part of the ice matrix.

Numerous studies have found wind-blown diatoms in fresh snow samples (Budgeon et al., 2012), exposed surfaces and in  
Antarctic ice cores (Burckle et al., 1988; Kellogg and Kellogg, 1996; Delmonte et al., 2013; Barrett 2013; Delmonte et al.,  
2017; Allen et al., 2020; Tetzner et al., 2021a). Recently, Allen et al. (2020) presented preliminary evidence that diatoms  
35 recovered from an Ellsworth Land (EL) ice core may provide a novel proxy of past south westerly wind (SWW) strength  
over the SO. Despite the potential the diatom record has shown to reconstruct past wind strength, this proxy has only been  
evaluated on a single site, without accounting for any regional variability. Moreover, recent findings reported by Tetzner et  
al. (2021a) suggest the diatom record preserved in ice cores from the Antarctic Peninsula (AP) exhibit intra-annual variations  
which could potentially dominate the annual signal, highlighting the need to study both annual and sub annual variability.

In this study, we present the diatom records from four shallow depth ice cores drilled between 2006 and 2020 in the AP and  
40 EL regions (Figure 1). Annual and sub-annual records of diatom abundance, concentration and assemblage composition are  
used to determine the regional and temporal variability of diatom content across the four sites. Ecological associations of the  
diatoms present are used to identify likely source regions and potential transport pathways.

## 2 Regional Settings

The Antarctic continent and the Ocean surrounding it present a region of contrasting environmental conditions. This section  
45 describes the main environmental features present in the AP-EL region and in the neighbouring Amundsen-Bellinghshausen  
Seas (ABS).

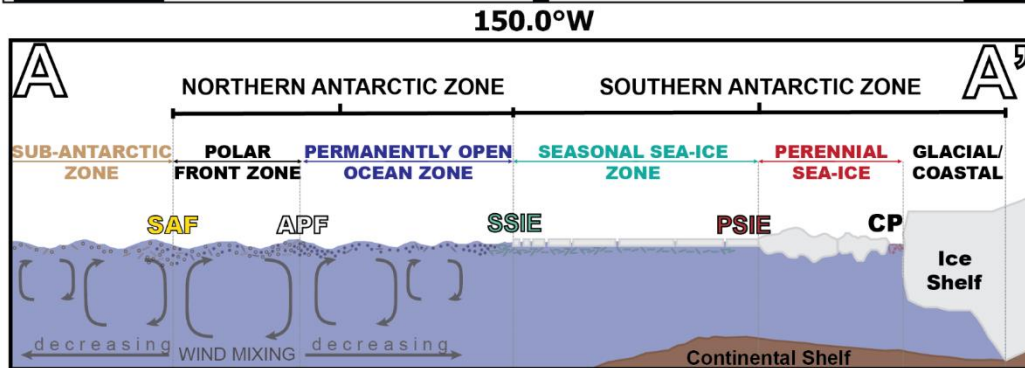
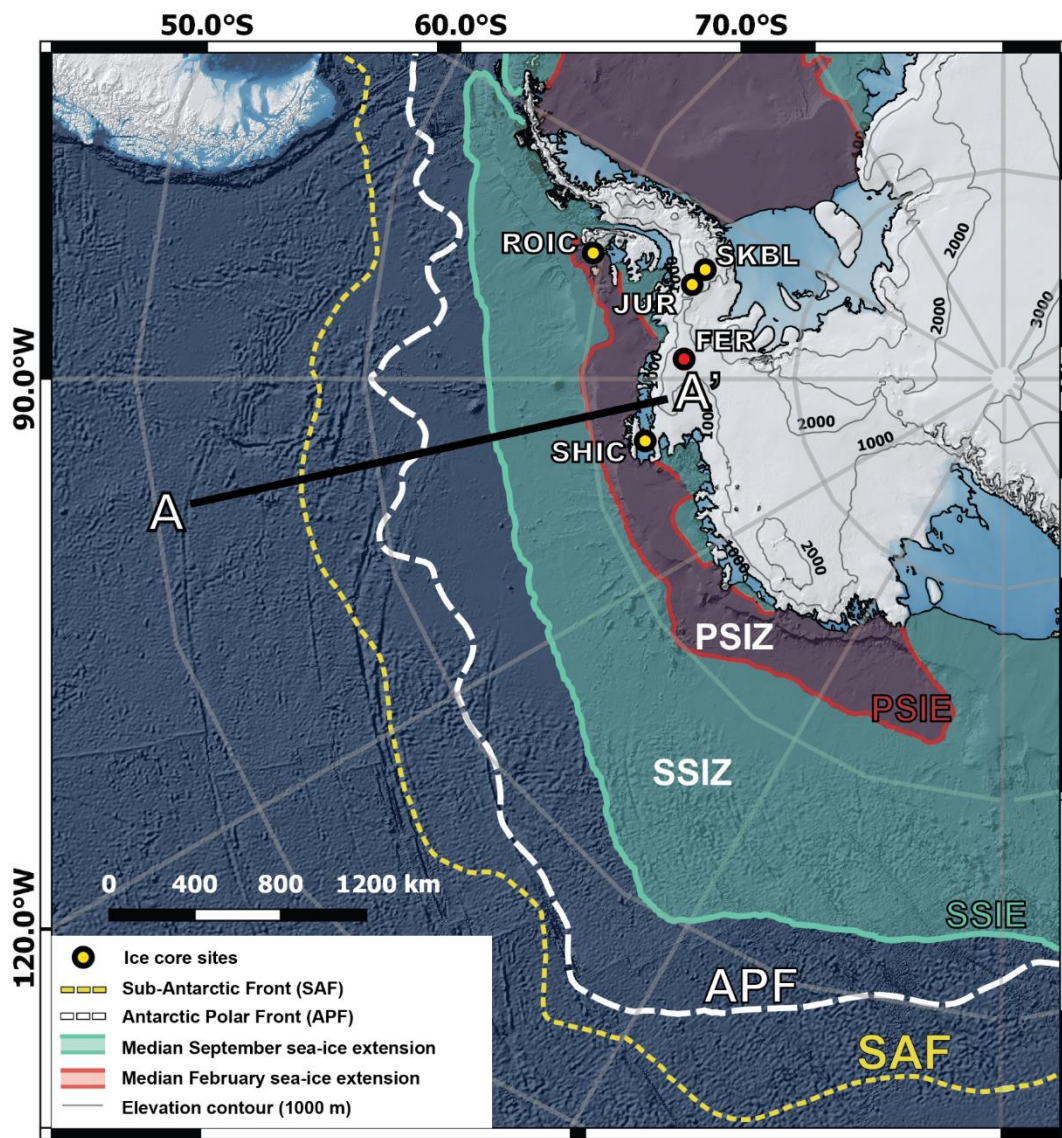
### 2.1 Oceanography

The SO is a vast circumpolar region that encompasses the southern-most basins of the Atlantic, Indian and Pacific Oceans.  
Zonally, the SO can be sub-divided into two major circum-Antarctic regions delineated by the presence of oceanographic  
50 fronts and sea ice cover: The Northern Antarctic Zone (NAZ) and the Southern Antarctic Zone (SAZ) (Figure 1). The NAZ  
is characterized by year-round open waters, limited to the north by the Sub-Antarctic Front (SAF) and to the south by the  
maximum extent of seasonal sea ice cover. The SAZ is characterized by the presence and variability of seasonal sea ice  
cover, delineated by the austral winter sea ice maximum to the north and by the Antarctic coast to the south.

The SO is one of the most productive water masses on Earth. The spatial and temporal patterns of productivity are highly  
55 variable across the region but can be generalised into two regions that broadly coincide with the NAZ and SAZ (Arrigo et  
al., 2008; Soppa et al., 2016). Primary production in the NAZ is characterized by a moderate seasonal cycle, highest (lowest)  
during austral spring (winter) at 300–400 (50–70)  $\text{mg C m}^{-2} \text{ d}^{-1}$ , and fairly stable annual production with interannual  
variability of 3.5 % (Arrigo et al., 2008). Conversely, primary productivity in the SAZ presents a strong seasonal cycle  
characterised by short-lived, intense blooms during austral spring/summer ( $>1600 \text{ mg C m}^{-2} \text{ d}^{-1}$ ) (Rousseaux and Gregg,



60 2013; Arrigo et al., 2008; Soppa et al., 2016). These intense blooms are triggered by increasing light availability and melt-  
induced stratification during the austral spring and/or summer months (Soppa et al., 2016). The opposite happens during the  
austral winter, when productivity in the SAZ is at its lowest due to light limitation and the large area covered by sea ice  
(Arrigo et al., 1998). Interannual variability in SAZ primary productivity (>19%) is considerably higher than the interannual  
variability observed in the NAZ (3.5 %), mainly driven by changes in the distribution and timing of sea ice melt (Arrigo et  
65 al., 2008; Smith and Comiso, 2008).





70 **Figure 1. Map showing the ice core sites and oceanographic features considered in this study. The yellow circles show the locations of the four ice core sites. The red circle show the location of the Ferrigno ice core (Allen et al., 2020). The pale green line shows the median September sea ice extension between 1980-2010 AD and represents the Seasonal Sea Ice Edge (SSIE). The red line shows the median February sea ice extension between 1980-2010 AD, and represents the Perennial Sea Ice Edge (PSIE). A-A' presents a schematic cross-section including the standard oceanographic features across the Amundsen-Bellinghshausen Sea (Schematic cross-section adapted from Allen et al. (2011)). SAF= Sub-Antarctic Front. APF= Antarctic Polar Front. SSIZ= Seasonal Sea Ice Zone. PSIZ= Perennial Sea Ice Zone. CP= Coastal Polynya.**

## 2.2 Climate

75 Regional atmospheric circulation in the AP-EL and the neighbouring ABS is dominated by the Amundsen Sea Low (ASL) with SWW advecting warm and moist air from the southern Pacific Ocean towards the AP (Turner et al., 2013; Orr et al., 2004). When approaching the Antarctic Peninsula, airmasses are diverted south, producing a northerly wind flow. Once airmasses reach the Antarctic ice sheet, they are blocked and deflected to the east where the flow is enhanced by katabatic winds flowing downslope from the ice sheet interior. This easterly flow is known as the Antarctic coastal easterlies (Hazel and Stewart, 2019). Winds over the SO, including the ABS, present a clear seasonality with stronger winds during the austral winter and weaker winds during the austral summer (Yu et al., 2020, Thomas and Bracegirdle, 2015; van Wessem et al., 2015). During the satellite-era (1979-present), surface winds have strengthened across the AP-EL region (van Wessem et al., 2015), corresponding to the broader observation that the SWW have experienced the strongest positive trend worldwide (Young and Ribal, 2019).

85 Air temperatures present a regional gradient with temperatures decreasing with increasing latitude and elevation. This regional gradient leaves coastal regions particularly sensitive to positive degree days during the austral summer with surface melting mainly restricted to coastal areas below 400 m a.s.l. (van Wessem et al., 2015; van Wessem et al., 2016). Direct temperature measurements and regional atmospheric climate models show temperatures have followed a positive trend in the southern AP region during the second half of the XXth century (Gonzales and Fortuny, 2018) and a slightly negative trend in the EL region (van Wessem et al., 2015).

95 Precipitation in the AP-EL regions are relatively constant throughout the year, exhibiting slightly lower values during the austral summer (Thomas and Bracegirdle, 2015; van Wessem, 2016). A regional gradient of decreasing precipitation with increasing elevation is identified across the region (van Wessem et al., 2016). Precipitation patterns in the AP-EL region are not considerably influenced by the occurrence of extreme precipitation events (Turner et al., 2019). Ice core records have demonstrated the AP-EL region has experienced a long-term positive trend in snow accumulation over the XXth century (Thomas and Tetzner, 2018), with some sites even doubling their snow accumulation (Thomas et al., 2008).

## 2.3 Sea ice

100 The Antarctic sea ice cover exhibits a regular seasonal cycle presenting its maximum (minimum) surface extension during September (February) (Parkinson, 2019). During the satellite-era (1979-present), the total Antarctic sea ice area has increased between 1.0 and 1.5 % (Parkinson and Cavalieri, 2012; Parkinson, 2019). However, in the ABS sectors, there has



been a significant decrease in the total area covered by sea ice ( $-2.5\%$  per decade) (Parkinson, 2019). This has led to an earlier retreat and a delayed formation of the sea ice cover, which together have resulted in a 3-month extension to the austral summer ice-free season in the ABS (Stammerjohn et al., 2012).

### 3 Methods

#### 105 3.1 Ice core records and age scales

Four ice cores from the southern AP and EL were included in this study (Figure 1) (Table 1). The Sherman Island ice core (SHIC, 21.3 m) from the West Antarctic ice sheet coast, and the Sky-Blu ice core (SKBL, 21.8 m) from the vicinity of Sky-Blu Field Station, southern AP, were both drilled using a Kovacs hand-auger during the austral summer 2019/2020. The Rothschild ice core (ROIC, 11.1 m) from Rothschild Island, southern AP, was drilled using a Kovacs hand-auger during the  
 110 austral summer 2005/2006. The Jurassic core (JUR, 140 m) from an inland site of the English Coast, southern AP, was drilled using the BAS electromechanical drill during the austral summer 2012/2013. For SHIC, SKBL and JUR, an ice core chronology was established based on their hydrogen peroxide ( $\text{H}_2\text{O}_2$ ) annual cycle that is assumed to peak during the austral summer solstice and to exhibit its minimum during the austral winter (Frey et al., 2006; Thomas et al., 2008). Ice core  
 115 chronologies were resolved using the annual cycle of the non-sea salt component of major ions, such as non-sea salt sulphates ( $\text{nssSO}_4^{2-}$ ) (Piel et al., 2006), that is assumed to peak between November and January in this region (Pasteris et al., 2014; Thoen et al., 2018). This non-sea salt stratigraphy was further corroborated by the presence of volcanic tephra in the 2001 AD ice core layer (Tetzner et al., 2021b). The top 15 m of SKBL included in this work and the full SHIC core were dated back to 1999 AD, with an estimated dating error for the 1999-2020 AD interval of  $\pm 3$  months for each year and with  
 120 no accumulated error. For ROIC, the ice core was dated using the annual cycles of major ion concentrations, resulting in an age scale from 2002-2006 AD. All annual values are reported as the austral winter-to-winter phase.

125 **Table 1. Summary of each ice core geographical location and main features of the datasets analysed in this study. SIE= Sea Ice Edge(\*) - The distance from SIE reported corresponds to the median for years covering the data interval. September SIE values used for calculations were obtained as distance between the ice core site and the closest point in the northern limit of 15% sea ice cover. February SIE values used for calculations were obtained as the distance between the ice core site and the closest sea ice free region.**

Core name	Long	Lat	Elevation (m a.s.l.)	ANNUAL RECORD		SUB-ANNUAL RECORD		Total depth used (m)	Distance from SIE (km)*	
				Years (AD)	# samples	Years (AD)	# samples		Sept	Feb
JUR	-73.06	-74.33	1139	1992-2012	20	2002-2006	16	36.9	1045	140
SKBL	-71.59	-74.85	1419	1999-2019	20	2002-2006	32	15.0	1148	200
SHIC	-99.63	-72.67	474	1999-2019	20	2002-2006	16	21.3	753	130



---

ROIC	-72.6	-69.6	438	-	-	2002-2006	36	11.1	598	70
------	-------	-------	-----	---	---	-----------	----	------	-----	----

---

### 3.2 Sample preparation and analyses

All ice cores included in this study were cut, using a band-saw with a steel blade, to obtain up to four ice core strips. The first strip (2 x 4 cm) was sub-sampled at 5 cm resolution and processed for ion chromatographic analyses of major ions and Methanesulphonic Acid (MSA) using a reagent-free Dionex ICS-2500 anion and IC 2000 cation system in a class-100 cleanroom.

A second ice core strip (3.3 x 3.3 cm) was cut from SHIC, SKBL and JUR and then melted using a Continuous Flow Analysis (CFA) system (Rothlisberger et al., 2000) in the ice chemistry lab at the British Antarctic Survey, UK to analyse the hydrogen peroxide concentration using enzymatic fluorometry examined by a FIALab photomultiplier-FL detector through a 3 mm Suprasil flow cell.

A third ice core strip was used for the diatom analyses. For SHIC, SKBL and JUR, this third strip was cut at annual resolution and an additional fourth ice core strip was cut at sub-annual resolution. Sub-annual samples for SHIC and JUR were cut based on the position of the hydrogen peroxide austral summer maxima and austral winter minima. Each annual interval between the hydrogen peroxide maxima and minima in SHIC and JUR, was split to obtain four sub-annual samples per year. Sub-annual samples from SKBL were cut at 10 cm resolution (~7-8 samples per year). Sub-annual samples from ROIC were cut at 30 cm resolution (~9 samples per year). Seasons are reported as austral summer (December to February, DJF), austral autumn (March to May, MAM), austral winter (June to August, JJA) and austral spring (September to November, SON).

All diatom samples were processed and analysed following the method and recommendations presented in Tetzner et al. (2021a). Observations regarding diatom preservation were based on the characteristics of frustule dissolution and degradation described by Warnock and Scherer (2015). Diatom frustules and fragments with a long axis less than 5  $\mu\text{m}$  were excluded from the diatom counting and identification.

After processing, diatom counts per sample ( $n$ ) were transformed to diatom abundance ( $n \text{ t}^{-1}$ ), where “ $t$ ” represents the temporal resolution of each sample. To compare the magnitude of the diatom abundance in different ice core sites, diatom concentrations ( $n \text{ L}^{-1}$ ) were calculated by normalizing the diatom counts per sample ( $n$ ) with the meltwater volume ( $L$ ) filtered. All correlations reported in this work were calculated after detrending each dataset and were calculated using the Pearson’s linear correlation ( $R$ ). All timeseries linear correlations were calculated over a 20-year period (1992-2012 AD for JUR and 1999–2019 AD for SHIC and SKBL).

Diatom identification and ecological associations were based on Armand et al. (2005), Halse and Syvertsen (1996), Hasle and Syvertsen (1997), Cefarelli et al. (2010), Zielinski and Gersonde (1997) and references therein. Diatoms were identified to species level where possible or combined in genera/morphological groups. Among the diatoms identified as *F. cylindrus* it is noted that they may also include *F. nana* (distinguished from *F. cylindrus* by size as per Cefarelli et al., 2010).



Unidentified (ie. obscured, undiagnostic & indistinct ) diatoms were omitted from ecological associations and assemblage composition but were included in the total diatom counts (n). The assemblage composition was determined for each site from the identified species and groups with abundances higher than 2.0 % of the whole assemblage and present in at least two samples of the 20 year record. Ecological associations were determined for the most abundant species/groups of each core. For the three 20-year diatom records (SHIC, JUR and SKBL), the assemblage composition was analysed over the whole period and for the two decadal subsets. The decadal subsets were produced to study temporal changes in diatom relative abundance and concentration over shorter timescales in order to assess the consistency of the assemblage. The assemblage composition at ROIC was only analysed over the 4-year period (2002-2006 AD). Sub-annual comparisons of the diatom relative abundance and diatom concentration were made over the common overlapping interval for all four sites (January 2002- January 2006 AD) (Table 1) to analyse the regional intra-annual variations in the diatom record. A Sea Ice Diatom Index (SIDI) was calculated for each sub-annual sample as the sum of the diatom concentrations of the two characteristic sea ice diatoms in the SO: *F. cylindrus* and *F.curta* (Lizotte, 2001). The SIDI from each ice core site was analysed over the overlapping period to study the relation between the total diatom concentration and the sea ice diatom concentration.

### 3.3 Sea ice extension data

Sea ice extension data were obtained from the satellite derived Sea Ice Index, Version 3 dataset (Fetterer et al., 2017) from the National Snow and Ice Data Centre (NSIDC). The Sea Ice Index provides monthly data on sea ice concentrations available at 25 km resolution from 1979 onward. September sea ice limits (defined as the median northerly extent of 15 % sea ice cover) were considered as the annual sea ice maximum, while February sea ice limits (defined as the median northerly extent of 15 % sea ice cover) were considered as the annual sea ice minimum (Thomas et al., 2019).

## 4 Results

A total of 4437 diatom valves and fragments were found among all samples. Of them, 2811 were found in annual samples, while 1626 were found in sub-annual samples. Diatoms were well preserved, with no evidence of dissolution in their structure, preserving delicate ornamentation and occurring as colonies of up to five cells. No clear trend was identified in the proportion of fragments relative to diatom frustules down-core. The main features and basic statistics of the diatom record for each ice core site are presented in Table 2.

A total of 25 diatom species and generic/taxa groupings were identified among all ice core sites. Of them, ten occurred at >2 % relative abundance in at least two samples of an ice core. Of these ten main taxa, six were present in more than one site, four were present in samples across all four ice core sites and four occurred exclusively at one site. Table 3 presents the relative abundance data for the ten main taxa in each ice core. Table 4 presents the basic statistics of the annual diatom abundance and concentration for each ice core site.





190

**Table 2.** Main features and basic statistics of the annual and sub-annual diatom records for each ice core. \*Calculations excluding austral spring 2002 AD. +Annual ROIC values were calculated combining sub-annual samples based on ROIC chronology (See section 2.1).

Core name	Number of samples	Total Diatom counts (n)	Total diatoms classifiable	Total volume filtered (L)	Mean volume filtered ( $\bar{x} \pm \text{s.d.}$ )
<b>Annual record</b>					
SHIC	20	1087	822	5.76	0.288 ± 0.069
JUR	20	1140	544	6.89	0.345 ± 0.079
SKBL	20	584	475	5.05	0.252 ± 0.086
ROIC <sup>+</sup>	4	665	435	3.78	0.943 ± 0.186
<b>Sub-annual record (2002-2006 AD)</b>					
SHIC	16	594	499	1.69	0.106 ± 0.03
JUR*	16	226	91	1.33	0.089 ± 0.014
SKBL	32	164	42	2.92	0.091 ± 0.007
ROIC	36	665	435	3.78	0.105 ± 0.014

195

**Table 3.** Relative abundance (%) and frequency (# of samples) of main diatom taxa in annual and sub-annual diatom records for each ice core. (\*) specimens of *Cyclotella* sensu lato (including *Lindavia*, *Discostella*, *Tertiarius* and *Pantocsekiella*). n represents the total number of samples in each sub-annual record. (s)= sea ice affiliated diatom. (o-SSIE)= open ocean – Seasonal Sea Ice Edge affiliated diatom. (o-POOZ)= open ocean – Permanently Open Ocean Zone affiliated diatom species/group.

	SHIC (1999-2019 AD)	JUR (1992-2012 AD)	SKBL (1999-2019 AD)	ROIC
<b>Annual record</b>				
<i>Fragilariopsis cylindrus</i> (s)	63.7 % (20)	18.2 % (14)	21.3 % (15)	-
<i>Shionodiscus gracilis</i> (o-SSIE)	18.5 % (18)	17.6 % (17)	10.9 % (10)	-
<i>Fragilariopsis curta</i> (s)	4.1 % (10)	-	-	-
<i>Fragilariopsis pseudonana</i> (o-POOZ)	3.6 % (11)	9.2 % (11)	15.3 % (10)	-
<i>Cyclotella</i> group*	6.8 % (19)	29.1 % (19)	37.2 % (20)	-
<i>Thalassiothrix</i> group (o-POOZ)	-	-	-	-
<i>Navicula</i> group	-	7.4 % (12)	-	-
<i>Nitzschia</i> group	-	-	6 % (12)	-



<i>Pseudonitzschia</i> spp. (o-POOZ)	3.3 % (10)	6.5 % (7)	9.3 % (8)	-
<i>Achnanthes</i> group	-	11.9 % (10)	-	-
<b>Sub-annual record (2002-2006 AD)</b>	<b>(n=16)</b>	<b>(n=16)</b>	<b>(n=32)</b>	<b>(n=36)</b>
<i>Fragilariopsis cylindrus</i> (s)	73.8 % (14)	34 % (11)	23.1 % (4)	83 % (21)
<i>Shionodiscus gracilis</i> (o-SSIE)	7.1 % (7)	8.8 % (4)	7.7 % (2)	6.5 % (11)
<i>Fragilariopsis curta</i> (s)	8.1 % (6)	-	-	4 % (10)
<i>Fragilariopsis pseudonana</i> (o-POOZ)	4.2 % (4)	14.3 % (4)	3.8 % (1)	2.5 % (6)
<i>Cyclotella</i> group*	3.1 % (6)	21.1 % (13)	34.6 % (5)	2 % (6)
<i>Thalassiothrix</i> group (o-POOZ)	-	-	-	2 % (6)
<i>Navicula</i> group	-	6.8 % (5)	-	-
<i>Nitzschia</i> group	-	-	7.7 % (2)	-
<i>Pseudonitzschia</i> spp. (o-POOZ)	3.7 % (6)	15 % (7)	23.1 % (5)	-
<i>Achnanthes</i> group	-	-	-	-

**Table 4.** Basic statistics for the diatom abundance and diatom concentration records from each ice core. \*Calculations excluding austral spring 2002 AD. +Annual ROIC values were calculated combining sub-annual samples based on ROIC chronology (See section 2.1).

Core Name	Time Interval (AD)	Diatom abundance (n y <sup>-1</sup> )			Diatom concentration (n L <sup>-1</sup> )		
		Mean (± s.d.)	Max	Min	Mean (± s.d.)	Max	Min
<b>Annual record</b>							
SHIC	1999-2019	54.4 (33.7)	110	10	188.9 (110.0)	376.3	41.8
JUR	1992-2012	57.0 (34.0)	166	20	180.7 (143.7)	723.0	52.5
SKBL	1999-2019	29.2 (14.9)	77	15	130.4 (72.1)	304.4	51.8
ROIC <sup>+</sup>	2002-2006	166.3 (42.1)	226	129	181.4 (52.0)	230.1	111.2
<b>Sub-annual record</b>							
SHIC	2002-2006	37.1 (50.1)	170	4	431.1 (671.2)	2538.1	34.8
JUR*	2002-2006	15.1 (5.8)	25	7	168.3 (58.1)	303.4	102.1
SKBL	2002-2006	5.1 (2.9)	13	1	56.3 (31.4)	148.7	10.3



---

ROIC	2002-2006	18.5 (19.1)	89	0	178.2 (177.3)	831.4	0
------	-----------	-------------	----	---	---------------	-------	---

---

200

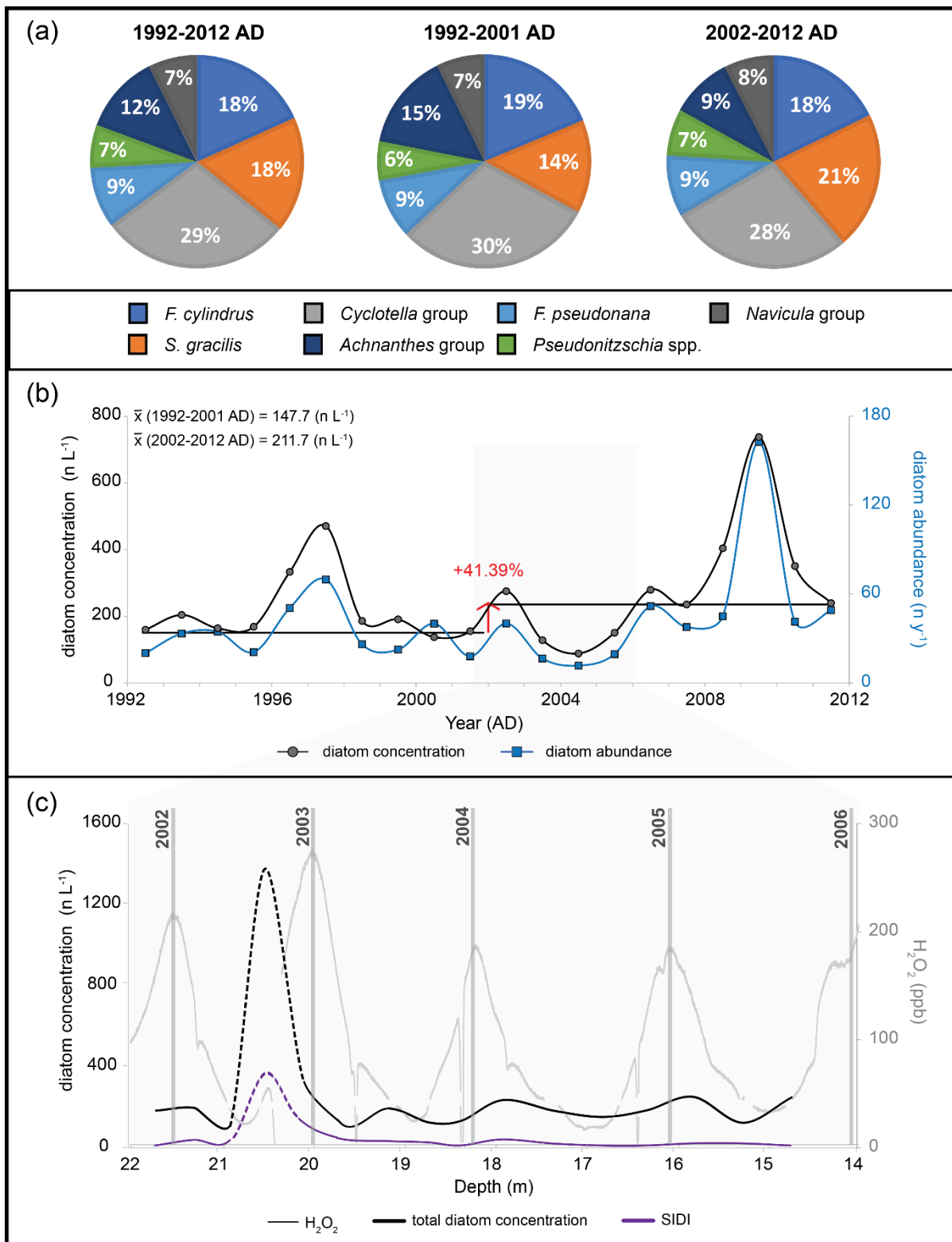
## 4.1 Jurassic ice core (JUR)

### 4.1.1 Diatom record

A total of 1140 diatom valves and fragments were identified in the JUR annual record (Table 2). The mean annual diatom abundance was  $57 \pm 34$  n y<sup>-1</sup>, with annual diatom abundance values ranging from 20 n y<sup>-1</sup> (2004-2005 AD) to 166 n y<sup>-1</sup> (2009-2010 AD) (Figure 2b) (Table 4). Diatom abundance is not correlated with the volume of meltwater filtered per sample (R=-0.19, p>0.05) or with the annual snow accumulation estimated from the ice core (R=-0.32, p>0.05). Mean annual diatom concentration was  $180.7 \pm 143.7$  n L<sup>-1</sup>, with annual diatom concentration values ranging from 52.5 n L<sup>-1</sup> (2004-2005 AD) to 723 n L<sup>-1</sup> (2009-2010 AD) (Figure 2b) (Table 4). The diatom concentration record exhibited a positive trend of 8.25 n L<sup>-1</sup> y<sup>-1</sup> (p=0.14) over the 1992-2012 AD period with mean diatom concentrations 41.39% higher between 2002-2012 AD (compared with 1992-2002) (Figure 2b).

The sub-annual diatom record from JUR exhibited uniform diatom concentration values and a single, major, increase during the austral spring 2002 AD ( $1383.3$  n L<sup>-1</sup>). Since this sample increase was more than five times higher than the mean diatom concentration over the whole 2002-2006 AD period ( $244.3 \pm 308.9$  n L<sup>-1</sup>) and not evident in the 20 year annual record of JUR, we consider this single major increase anomalous and exclude it from the sub-annual calculations. Excluding the increase identified during the austral spring of 2002 AD, the mean diatom concentration was  $168.3 \pm 58.1$  n L<sup>-1</sup>, showing moderate variations for 2003-2005 AD and no clear seasonality (Figure 2c).

Of the 1140 diatoms counted in the annual diatom record of the JUR ice core, 544 were identified to genus level or higher. Seven species/taxa groupings occur at >2% in at least two samples with highest relative abundances of *Shionodiscus gracilis* (17.6%), *Fragilariopsis cylindrus* (18.2%), and the *Cyclotella* group (29.1%) (Table 3). Decadal subsets show minor discrepancies, only exhibiting a 7% increase in the abundance of *S. gracilis* and a 6% decrease in the abundance of *Achnanthes* group in the most recent decade (2002-2012 AD) (Figure 2a). Sub-annual samples showed no clear seasonality in the distribution of the SIDI over the 2002-2006 AD period (Figure 2c).





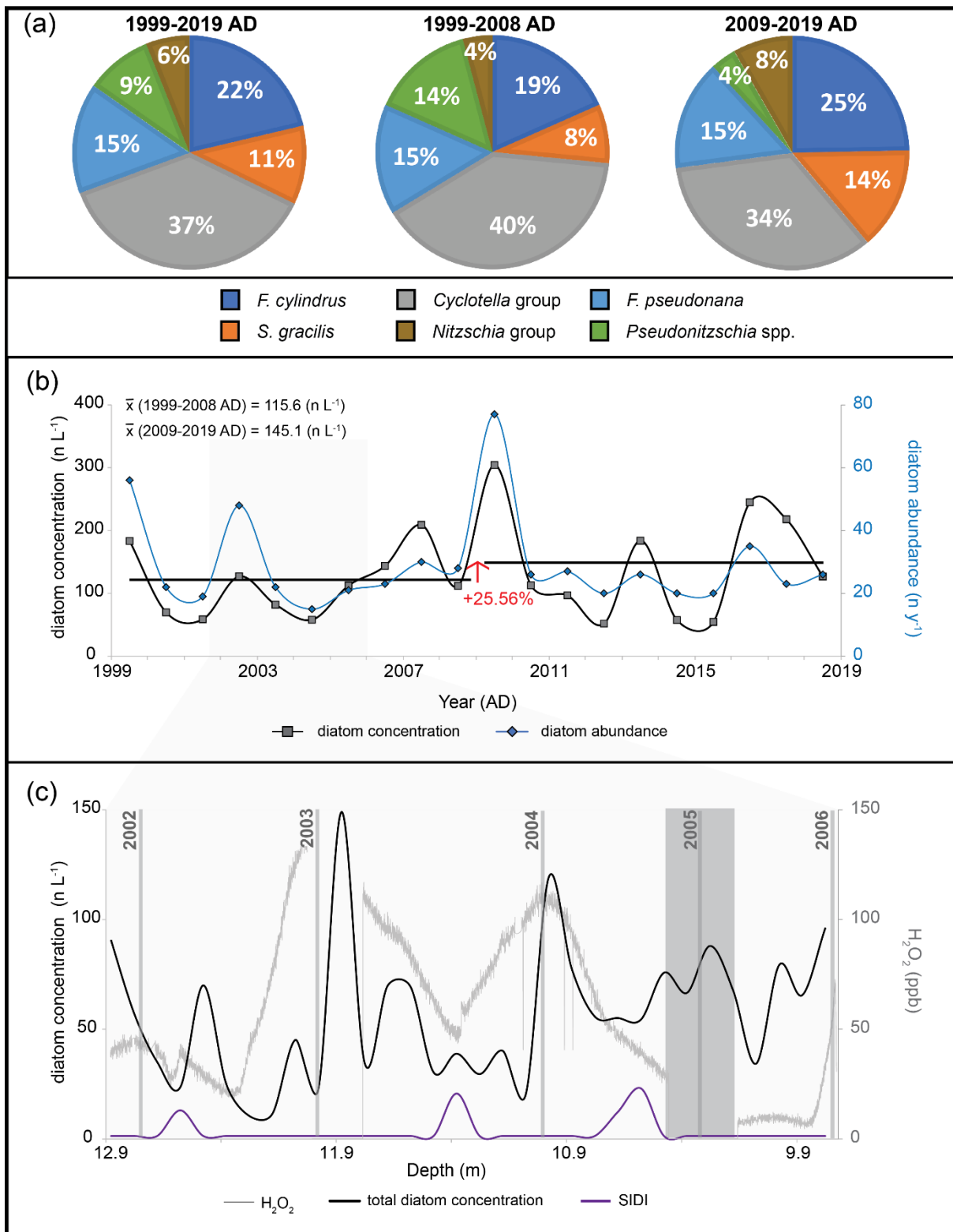
225 **Figure 2. Diatom record from the JUR ice core. a) Main diatom assemblage composition of the JUR ice core during 1992-2012 AD and during decadal subsets. Percentages reported in this figure were normalized to the main species identified. b) diatom concentration and diatom abundance timeseries. The red arrow represents the percentual variation in the diatom concentration decadal mean. c) Total diatom concentration and SIDI variations down-core for the 2002-2006 AD horizon. Vertical grey lines indicate temporal horizons based on the austral summer maxima in H<sub>2</sub>O<sub>2</sub>.**

## 4.2 Sky-Blu ice core (SKBL)

### 230 4.2.1 Diatom record

A total of 584 diatom valves and fragments were identified in SKBL (Table 2). A mean annual diatom abundance of  $29.2 \pm 14.9 \text{ n y}^{-1}$  was obtained, with values ranging from  $15 \text{ n y}^{-1}$  (2009-2010 AD) to  $77 \text{ n y}^{-1}$  (2004-2005 AD) (Figure 3b) (Table 4). No correlation is observed between the diatom abundance and either the volume of meltwater filtered per sample ( $R=-0.01$ ,  $p>0.05$ ) or the annual snow accumulation estimated from the ice core ( $R=-0.03$ ,  $p>0.05$ ). Mean annual diatom  
235 concentration was  $115.6 \pm 72.1 \text{ n L}^{-1}$ , with values ranging from  $51.8 \text{ n L}^{-1}$  (2012-2013 AD) to  $304.4 \text{ n L}^{-1}$  (2009-2010 AD) (Figure 3b) (Table 4). The annual diatom concentration record presented a positive trend of  $2.56 \text{ n L}^{-1} \text{ y}^{-1}$  ( $p=0.37$ ) over the 1999-2019 AD period with an increase of 25.56% from a mean concentration of  $115.6 \text{ n L}^{-1}$  for 1999-2008 AD, to  $145.1 \text{ n L}^{-1}$  for 2009-2019 AD (Figure 3b). SKBL sub-annual diatom concentrations (mean= $56.3 \pm 34.4 \text{ n L}^{-1}$ ) presented modest variations throughout the year with slightly higher concentrations consistently during late austral summer/early autumn  
240 (Figure 3c).

Among the 584 diatoms counted in SKBL, 475 were classified to genus level or higher. Six species/taxa groupings were present at  $>2\%$  in at least two samples (Table 3). with highest relative abundances of *S. gracilis* (10.9%), *F. pseudonana* (15.3%), *F. cylindrus* (21.3%) and the *Cyclotella* group (37.2%). The most recent decade (2009-2019 AD) exhibited a decrease of 10% and 6% in the relative abundance of *Pseudonitzschia* spp. and the *Cyclotella* group, respectively and a 6%  
245 increase of both *S. gracilis* and *F. cylindrus* (Figure 3a). Sub-annual samples revealed no clear seasonality in the distribution of SIDI nor in-phase variability between SIDI and the total diatom counts over the 2002-2006 AD period (Figure 3c).





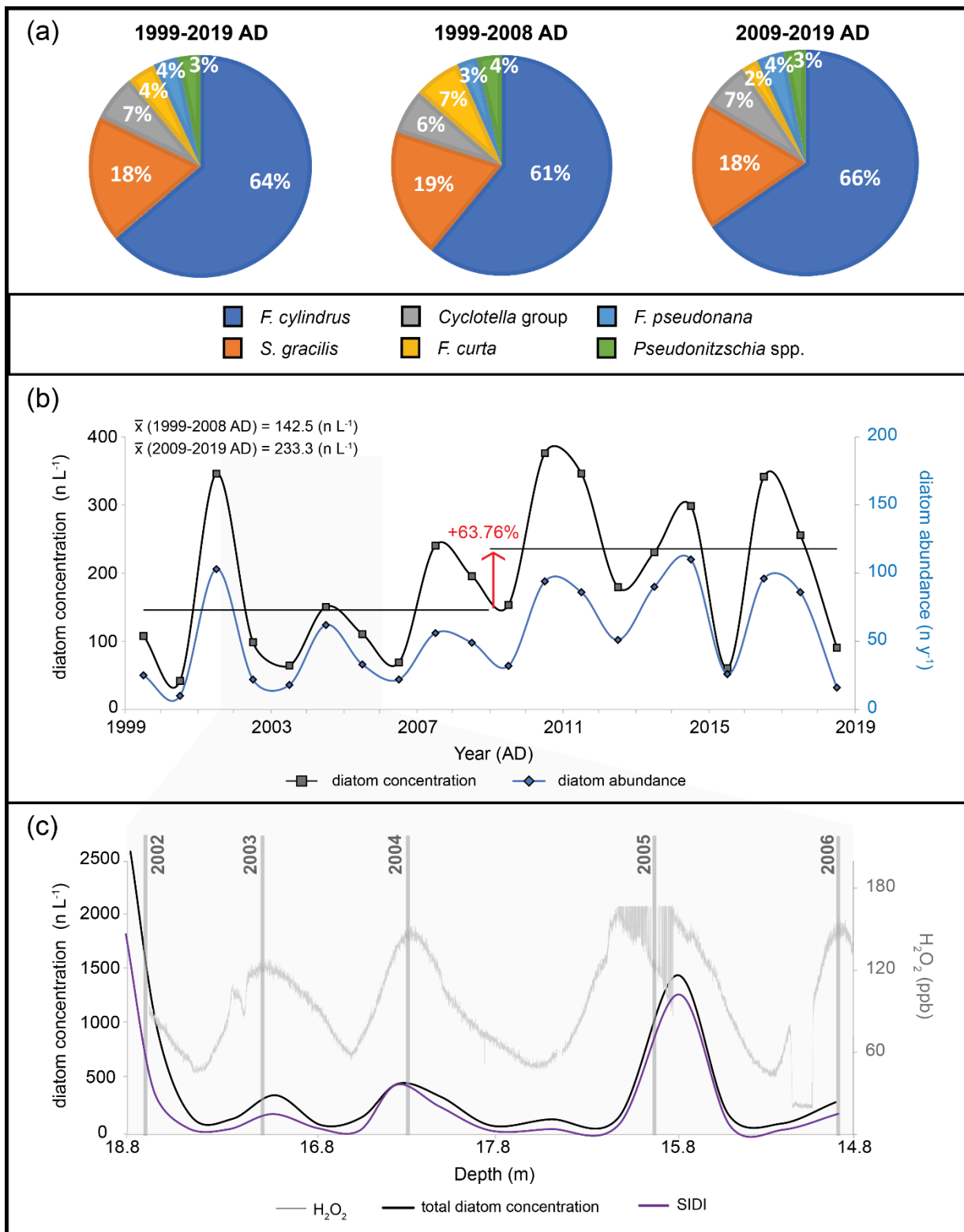
250 **Figure 3. Diatom record from the SKBL ice core. a) Main diatom assemblage composition of the SKBL ice core during 1999-2019 AD and during decadal subsets. Percentages reported in this figure were normalized to the main species identified. b) diatom concentration and diatom abundance timeseries. The red arrow represents the percentual variation in the diatom concentration decadal mean. c) Total diatom concentration and SIDI variations down-core for the 2002-2006 AD horizon. Vertical grey lines indicate temporal horizons based on the austral summer maxima in H<sub>2</sub>O<sub>2</sub>. Vertical grey band indicates a gap in the H<sub>2</sub>O<sub>2</sub> dataset.**

### 4.3 Sherman Island ice core (SHIC)

#### 4.3.1 Diatom record

255 The annual diatom record from SHIC comprised 1087 diatom valves and fragments (Table 2). The annual diatom abundance presented a mean value of  $54.4 \pm 33.7 \text{ n y}^{-1}$ , with annual values ranging from  $10 \text{ n y}^{-1}$  (2000-2001 AD) to  $110 \text{ n y}^{-1}$  (2014-2015 AD) (Figure 4b) (Table 4). A weak but not statistically significant correlation is observed between diatom abundance and meltwater filtered per sample ( $R=0.28$ ,  $p>0.05$ ), while no correlation is observed with the annual snow accumulation estimated from the ice core ( $R=-0.09$ ,  $p>0.05$ ). Mean annual diatom concentration was  $188.9 \pm 110 \text{ n L}^{-1}$ , with values  
260 ranging from  $41.8 \text{ n L}^{-1}$  (2000-2001 AD) to  $376.3 \text{ n L}^{-1}$  (2010-2011 AD) (Figure 4b) (Table 4). The annual diatom concentration record presented a positive trend of  $6.23 \text{ n L}^{-1} \text{ y}^{-1}$  ( $p=0.15$ ) over the 1999-2019 AD period. Decadal subset analyses showed an increase in the mean annual diatom concentration of 63.76% from  $142.5 \text{ n L}^{-1}$  (1999-2008 AD) to  $233.3 \text{ n L}^{-1}$  (2009-2019 AD) (Figure 4b). The sub-annual diatom concentration record from SHIC exhibited a clear seasonal pattern characterized by higher values ( $>300 \text{ n L}^{-1}$ ) during austral summer/early autumn, and lower values ( $<100 \text{ n L}^{-1}$ ) during  
265 austral winter/early spring (Figure 4c).

Of the 1087 diatoms counted in SHIC, 822 were identified to genus level or higher. Six species/taxa groupings occurred  $>2\%$  in at least two samples of SHIC, with *F. cylindrus* (63.7%) and *S. gracilics* (18.5%) accounting for more than 82% of the diatoms identified at SHIC (Table 3). Decadal subsets from the main diatom assemblage show minor variations, the largest being a 5% decrease (increase) in the relative abundance of *F. curta* (*F.cylindrus*) in the most recent decade (2009-  
270 2019 AD) (Figure 4a). Sub-annual samples from SHIC exhibited seasonality in the distribution of the SIDI, in-phase with the seasonality described by the total diatom counts over the 2002-2006 AD period (Figure 4c).







275 **Figure 4. Diatom record from the SHIC ice core. a) Main diatom assemblage composition of the SHIC ice core during 1999-2019 AD and during decadal subsets. Percentages reported in this figure were normalized to the main species identified. b) diatom concentration and diatom abundance timeseries. The red arrow represents the percentual variation in the diatom concentration decadal mean. c) Total diatom concentration and SIDI variations down-core for the 2002-2006 AD horizon. Vertical grey lines indicate temporal horizons based on the austral summer maxima in H<sub>2</sub>O<sub>2</sub>.**

#### 4.4 Rothschild ice core (ROIC)

##### 4.4.1 Diatom record

280 The diatom record from ROIC comprised 665 diatom valves and fragments (Table 2). The annual diatom abundance presented a mean value of  $166.3 \pm 42.1 \text{ n y}^{-1}$ , with values ranging from  $129 \text{ n y}^{-1}$  (2002 AD) to  $226 \text{ n y}^{-1}$  (2003 AD) (Table 4). Diatom abundance is not correlated with volume of meltwater filtered per sample ( $R=0.10$ ,  $p>0.05$ ). The annual diatom concentration presented a mean value of  $176.1 \pm 52 \text{ n L}^{-1}$ , with values ranging from  $111.2 \text{ n L}^{-1}$  (2002 AD) to  $230.1 \text{ n L}^{-1}$  (2003 AD) (Table 4). The sub-annual diatom concentration from ROIC revealed a strong seasonality, with higher values  
285 ( $>250 \text{ n L}^{-1}$ ) during austral summer/early autumn, and lower values ( $<70 \text{ n L}^{-1}$ ) during austral winter/early spring (Figure 5b).

Among the 665 diatoms counted in ROIC, 435 were identified to genus level or higher. The assemblage included six diatom species/taxa, dominated by *F. cylindrus* (83%) with minor presence of *S. gracilis* (6.5%) and *F. curta* (4%) (Figure 5a) (Table 3). Sub-annual samples from ROIC presented a clear seasonality in the distribution of SIDI, in-phase with the  
290 seasonal pattern identified in the total diatom counts over the 2002-2006 AD period (Figure 5b).

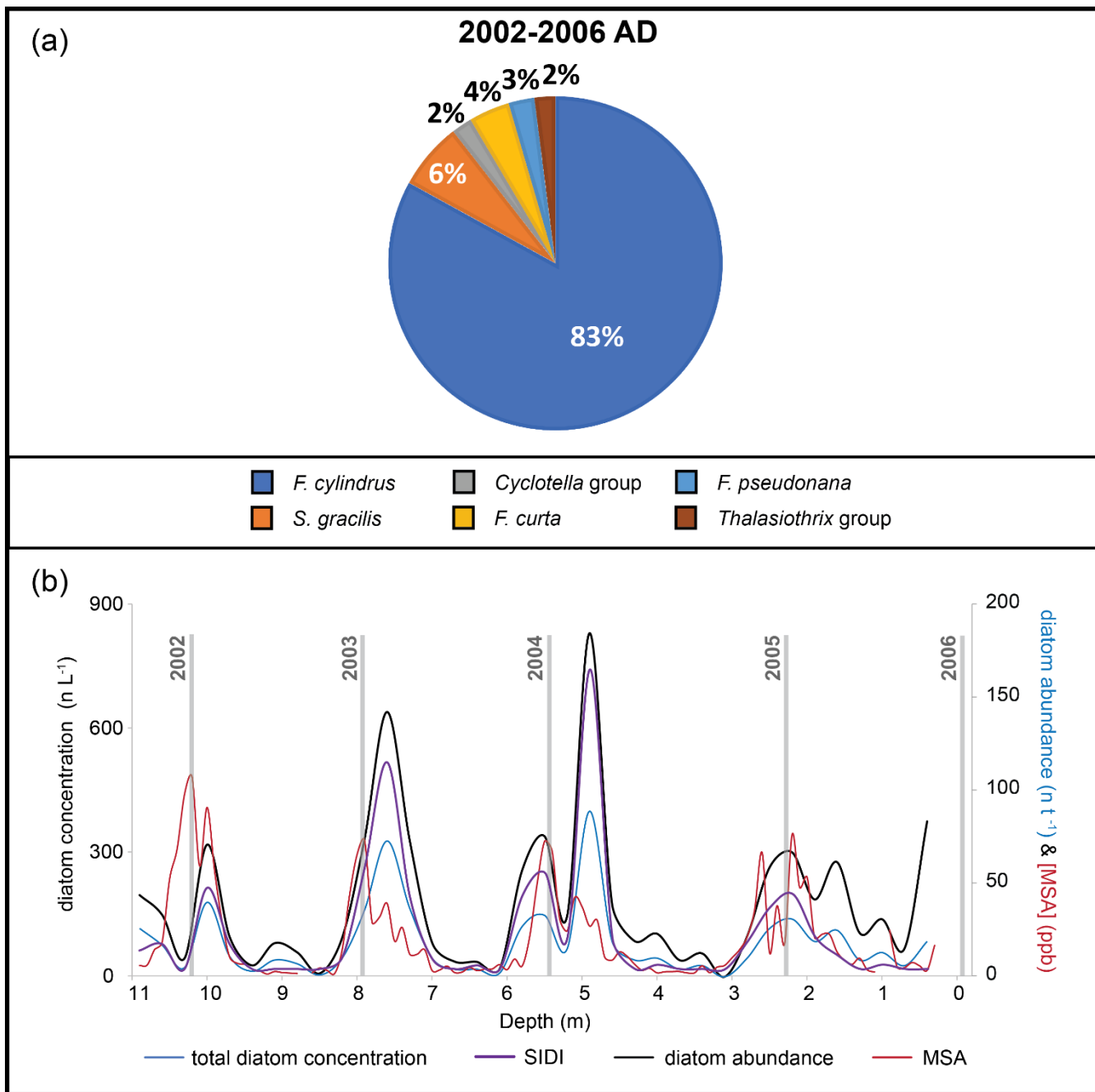


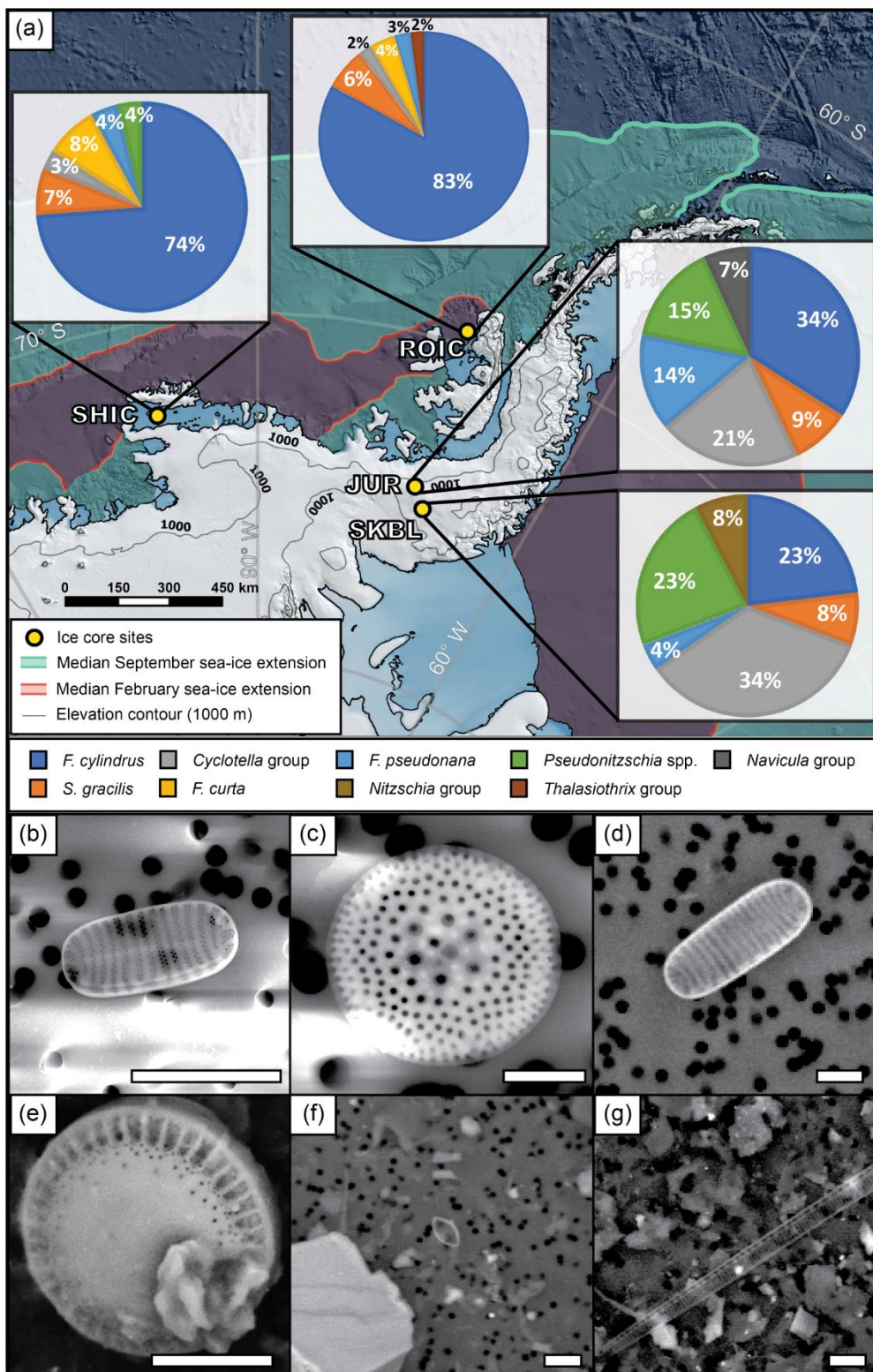
**Figure 5. Diatom record from the ROIC ice core. a) Main diatom assemblage composition of the ROIC ice core (2002-2006 AD). Percentages reported in this figure were normalized to the main species identified. b) Total diatom concentration, total diatom abundance and SIDI variations down-core for the 2002-2006 AD horizon. Vertical grey lines indicate temporal horizons based on the austral summer maxima in MSA.**



#### 4.5. Regional diatom ecology

The diatom assemblages at all sites is dominated by *Fragilariopsis* spp. and *Shionodiscus* spp., two genera that are common and abundant in the SO (Crosta et al., 2005; Rigual-Hernandez et al., 2015). An additional group identified in every ice core is the *Cyclotella* group, that is comprised of unspecified specimens of *Cyclotella sensu lato* (including *Lindavia*, *Discostella*,  
300 *Tertiarius* and *Pantocsekiella*), a cosmopolitan genus-complex with broad ecological affinities across marine, brackish and freshwater environments (Lowe, 1975).

Out of the ten taxa identified in the main diatom assemblages (Table 3), six are exclusively marine, whilst the other four have been identified in marine, brackish and freshwater environments (Lowe, 1975; Van de Vijver and Beyens, 1999; Bouchard et al., 2004; Hamsher et al., 2016; Malviya et al., 2016). The marine taxa include sea ice affiliated diatoms (*F. cylindrus* & *F. curta*) (Zielinski and Gersonde, 1997; Lizotte, 2001) and open ocean species/groups (*S. gracilis*, *F. pseudonana*, *Pseudo-nitzschia* spp. & *Thalassiothrix* gp) (Crosta et al., 2005; Zielinski and Gersonde, 1997; Rigual-Hernandez et al., 2015). In total, the marine taxa contribute at least 58% to the assemblages of the four ice core sites and indicate a predominantly marine origin for the diatoms present in the AP and EL ice cores (Figure 6).  
305





310 **Figure 6. Main diatom assemblage for each ice core over their overlapping period (2002-2006 AD). a) Map of ice core sites showing the main diatom assemblage for each location. Scanning Electron Microscope (SEM) micrographs of the most abundant diatom taxa b) *F. cylindrus* found in ROIC. c) *S. gracilis* found in JUR. d) *F. curta* found in SHIC. e) Diatom valve as example of the *Cyclotella* group found in JUR. f) *F. pseudonana* found in JUR. g) *Pseudonitzschia* spp. found in SKBL. Scale bar in bottom right of each frame represents five microns.**

#### 315 **4.6 Regional distribution**

The diatom concentration records from the four ice cores were compared for the overlapping period (2002-2006 AD). The diatom concentration showed a difference between higher mean diatom concentrations at ROIC (178.2 n L<sup>-1</sup>) and SHIC (431.1 n L<sup>-1</sup>) than at JUR (168.3 n L<sup>-1</sup>) and SKBL (56.3 n L<sup>-1</sup>). Diatom concentration in ROIC and SHIC were characterized by higher values (>250 n L<sup>-1</sup> & >300 n L<sup>-1</sup> respectively) during austral summer/early autumn, and lower values (<70 n L<sup>-1</sup> & <100 n L<sup>-1</sup> respectively) during austral winter/early spring. Conversely, the diatom concentration at JUR and SKBL of 168.3 ± 46 n L<sup>-1</sup> and 56.3 ± 31.4 n L<sup>-1</sup>, respectively exhibit only minor variations throughout the year and no obvious seasonality.

A regional comparison over the overlapping period (2002-2006 AD) shows the main diatom assemblage also differs across the region. Main diatom assemblages from ROIC and SHIC are dominated by *F. cylindrus* (≥73%) with other species representing minor percentages of the main assemblage. Conversely, JUR and SKBL present three or more species which represent the main proportion of the assemblage. While *F. cylindrus* dominates the assemblage of ROIC and SHIC it contributes ≤34% on JUR and SKBL. The opposite was identified for the *Cyclotella* group where ROIC and SHIC contain ≤3%, while JUR and SKBL contain ≥21%. An additional division was identified in the presence of *F. curta*. This diatom species is widely identified and presents a similar proportion (~4-8%) in ROIC and SHIC, but it is absent in JUR and SKBL.

### 5. Discussion

#### 330 **5.1 Diatom source**

Regional diatom ecology reveal that the diatom record preserved in ice cores from the Southern AP and EL is almost exclusively dominated by marine taxa abundant in the SO (Crosta et al., 2005; Zielinski and Gersonde, 1997; Rigual-Hernandez et al., 2015). Marine diatoms have been previously found in numerous ice core sites in Antarctica and their source has been attributed to the SO (Burckle et al., 1988; Kellogg and Kellogg, 1996; Budgeon et al., 2012; Delmonte et al., 2013; Delmonte et al., 2017; Allen et al., 2020; Tetzner et al., 2021a). The marine diatoms analysed in this work were not only well persevered but also present in colonies. The recovery of fresh-looking specimens still articulated in short chains suggests a rapid transport of the cells directly from the source to the ice core sites. These findings support SO surface waters as the principal source of diatoms and aeolian transport as the mechanism to transfer diatoms to the AP and EL ice core sites. This is consistent with previous studies showing airmasses originated in the SO are transported within days to the AP and EL ice core sites (Thomas and Bracegirdle, 2015; Allen et al., 2020). Whilst the SO is the principal source of diatom to ice cores in this region, we cannot rule-out minor contributions from exposed sediments and fresh/brackish-water bodies.



The SO is a vast and diverse region covering major oceanographic zones with varied environmental conditions (Figure 1). Ecological affinities of the marine diatoms present in each ice core indicate the dominant oceanographic source region and suggest that the marine diatoms are principally derived from the SSIZ and the POOZ (See section 2).

345 The diatom assemblage of SHIC and ROIC are dominated by diatoms associated with the SSIZ ( $\geq 68\%$ , *F. cylindrus* and *F. curta*). A prevalent SSIZ source of diatoms for these two sites is also supported by the high mean diatom concentrations and the strong seasonal variability (Table 4), reflecting the typical intense, seasonal blooms that characterise the SSIZ (See section 2). The proximity of the diatom source region to the SHIC and ROIC may also contribute to the enhanced diatom concentrations at these two sites (Tesson et al., 2016) (Figure 1).

350 The diatom assemblages of JUR and SKBL are dominated by diatoms associated with the SSIZ and the POOZ ( $\geq 58\%$ ). Thus, suggesting both the SSIZ (within the SAZ) and the POOZ (within the NAZ) as the source of diatoms for these ice core sites. Despite both oceanographic zones being identified as diatom sources, two lines of evidence support the POOZ as the dominant source region. Compared with the ROIC and SHIC coastal ice cores, JUR and SKBL contain a lower proportion of sea ice diatoms ( $< 34\%$  &  $\leq 23.1\%$  respectively), suggesting reduced transport from the SSIZ. The comparatively higher

355 proportion of the more distally-sourced, open ocean diatoms denote greater transport from the NAZ (Figure 1). The sub-annual samples also support the POOZ within the NAZ as the main diatom source. The lack of seasonality detected in the JUR and SKBL sub-annual diatom records is consistent with the modest seasonality in primary production observed in the NAZ of the Pacific sector (Arrigo et al., 2008; Soppa et al., 2016). Moreover, the reduced concentration of sea ice diatoms (*F. cylindrus* & *F. curta*) and its lack of correlation with the variability of the total diatom concentration, suggests the SSIZ

360 plays a modest role in shaping the diatom record at these two sites (Figure 2c and Figure 3c). Overall, the JUR and SKBL diatom records indicate the POOZ (within the NAZ) as the primary source of diatoms to these sites, with limited contributions from the SSIZ.

The different source regions for the ROIC and SHIC versus the JUR and SKBL diatom records, is likely due to their locations. ROIC and SHIC are coastal, low elevation sites whilst JUR and SKBL are inland, high elevation sites. Back

365 trajectory analyses reveal that airmasses arriving at high elevation sites (JUR and SKBL) are in contact with the sea surface farther offshore, north of the SSIZ and therefore entrain mostly open ocean diatoms (Thomas and Bracegirdle, 2009; Thomas and Bracegirdle, 2015; Allen et al., 2020).

The identification of two different diatom source regions for ice core sites located in contrasting geographical locations is consistent with previous findings across Antarctica. A SSIZ source for coastal regions is consistent with previous findings

370 from a coastal site ( $\sim 400$  m a.s.l., 10km away from the coast and 50km from the ice-free ocean) in Windmill Island, East Antarctica (Budgeon et al., 2012). At this site, diatom concentrations ranged from 0-180 ( $n L^{-1}$ ) and the diatom main assemblage was almost exclusively composed of *F. cylindrus*, *F. curta*, *S. gracilis* and *F. pseudonana*. Similarly, our results from inland sites agree with the results obtained from the Ferrigno ice core, drilled at an inland location in EL (1354 m.a.s.l., 140 km away from the coast) (Allen et al., 2020). At this site, an open water region within the NAZ was identified as the

375 dominant diatom source and diatom concentration values (0-140  $n L^{-1}$ ) were comparable to the values obtained for JUR and



380 SKBL. The dominance of marine diatoms preserved in the records from inland high-elevation sites in the AP and EL region (JUR, SKBL and FER) contrasts with the predominance of freshwater and reworked diatoms previously recorded in Antarctic ice cores from continental sites such as South Pole, Dome C and Vostok (Burckle et al., 1988; Kellogg and Kellogg, 1996; Kellogg and Kellogg, 2005). This disparity shows ice cores from the AP-EL region are uniquely situated to capture marine-transported diatoms.

## 5.2 Inter-annual variability

385 A first step in understanding the temporal variability in the diatom record is to examine the relative role of ice core site conditions and post-depositional processes. The lack of correlation between the diatom abundance, meltwater volume and ice core snow accumulation suggest that deposition of diatoms occurs under a mixed regime, which does not depend on precipitation changes at the ice core site. Similarly, no clear relationship was identified between the sub-annual diatom abundance and the monthly mean wind speed measured at JUR, SKBL and in the vicinities of ROIC (Tetzner et al., 2019). These results demonstrate that the magnitude and variability of the diatom records are not controlled by local environmental conditions at the ice core sites.

390 Similar results have been previously reported for the Ferrigno ice core site, where the annual diatom abundance presented a weak and non-significant correlation with the volume of meltwater filtered per sample ( $R=0.14$ ,  $p>0.05$ ) and with the annual snow accumulation ( $R=0.12$ ,  $p>0.05$ ) (Allen et al., 2020). Our results, and the results presented for the Ferrigno ice core, contrast with the depositional mechanisms of insoluble mineral dust over the ice sheets (Sudarchikova et al., 2015). In particular, insoluble mineral dust has been shown to be deposited either via wet (snow scavenging in the atmosphere) (Wolff et al., 1998; Breider et al., 2014), dry/wet (Koffman et al., 2014) or dry deposition (gravitational settling) (Li et al., 2010), depending on the location of the ice core site. Likewise, deposition of insoluble mineral dust has been shown to be enhanced under weak wind conditions, which favours the gravitational settling of dense particles (Fernandes et al., 2019). Both observations contrast with our results which show diatoms are not deposited under specific wind or precipitation regimes.

400 Whilst the potential effects of post-depositional processes such as snow ablation and redeposition cannot be ruled out (Lenaerts and Van den Broeke, 2012, van Wessem et al., 2016), the continuity and regularity seen in the  $H_2O_2$  seasonal cycle indicate that these ice core records were not disrupted by major ablation or redeposition events. Altogether, results presented in this work reveal that local environmental changes are not the main drivers of the temporal variability in the diatom record preserved in the AP & EL ice cores.

405 Decadal subset analyses of the diatom concentration revealed a regional increase of 41.39 %, 25.56 % and 63.76 % for JUR, SKBL and SHIC respectively, between the first and second decades. The consistent increase in diatom concentrations over the three sites suggests there may be a common driver of the temporal variability in the diatom record. Firn compaction affects every ice core site regardless of their location. Even though the continuous deposition of snow on the surface adds a progressive load on top of the diatoms preserved in deeper ice core layers, diatom frustules have shown to withstand pressures equivalent to 700 tonnes  $m^{-2}$  without fracturing (Hamm et al., 2003). Moreover, the recovery of fresh-looking



specimens still articulated in short chains and preserving delicate ornamentation at the bottom of these ice cores evidence the  
410 diatom records were not affected by mechanical fracturing or chemical dissolution downcore. Thus, proving the recent  
increase in the diatom concentration is not caused by post-depositional processes progressively affecting the diatom record  
down-core.

Decadal subset analyses of the diatom assemblages revealed only minor variations in composition (Figures 2a, 3a and 4a),  
confirming that the principal sources (POOZ and SSIZ) have remained stable over the last two-to-three decades. Since the  
415 diatom source areas have not moved, the recent increase in diatom concentration likely reflects environmental changes  
within the POOZ and SSIZ of the ABS (and/or transport efficiency). The SO/ABS has recently experienced considerable  
changes in atmospheric circulation and sea ice dynamics over recent decades (See section 2). The POOZ is located within  
the SWW belt and therefore prone to be affected by changes in the strength and position of the SWW (Mayewski et al.,  
2013; Menviel et al., 2018). Recent strengthening and southern shift in SWW as the potential driver of the increased diatom  
420 concentrations observed in JUR and SKBL is consistent with the strong correlation between the ice core diatom record and  
changes in wind strength over the SO reported by Allen et al. (2020). For the SHIC, the close link between the diatom record  
and the local SSIZ conditions (Arrigo et al., 2008; Arrigo et al., 2012) suggest that variations in the ABS SSIZ will be  
reflected in the SHIC diatom record. In particular, the recent decrease in the area of the ABS SSIZ (Parkinson, 2019) has  
shortened the distance between the SSIZ and the ice core sites. Similarly, the prolonged ice-free season (Stammerjohn et al.,  
425 2012) has extended the exposure of stratified waters in the SSIZ. Both, potentially increasing the availability of diatoms to  
be transported to SHIC. Altogether, the recent increase in diatom concentration across the region likely reflects the observed  
environmental changes within the POOZ and SSIZ.

## 6 Conclusions

Marine diatoms are faithful recorders of environmental conditions. Resolving the environmental controls on the assemblage  
430 and abundance variations of diatoms in different Antarctic ice cores offers the potential to establish a new and unique  
paleoenvironmental proxy. Our multi-site assessment of diatoms preserved in Antarctic Peninsula and Ellsworth Land ice  
cores confirm that the 20 year record is dominated by pristine specimens of Southern Ocean marine diatoms. Diatoms in the  
two coastal ice cores are dominated by sea ice taxa and exhibit consistent timing of peak inputs during austral summer. At  
inland sites, the diatom records are dominated by open ocean species with relatively constant inputs throughout the year.  
435 This strong geographical division can be exploited to recover valuable environmental information from both the sea ice and  
open ocean regions.

Diatom records from all four Antarctic Peninsula and Ellsworth Land ice cores reveal a recent rise in diatom concentrations.  
We demonstrate that this regional increase is not driven by changes in local conditions at the ice core sites or in the diatom  
sources, but is likely a result of stronger winds transporting more diatoms and/or declining sea ice extent reducing the





440 transport distance. Altogether, our findings emphasize how the diatom record preserved in Antarctic ice cores has the potential to become a robust proxy of environmental conditions in the Southern Ocean.

The strong seasonality of the diatom record at coastal sites also holds potential as a new chronological marker, providing a novel tool to date ice cores where the effects of climate change (e.g. Surface melt, increased rain events) impair traditional annual layer counting (Simoes et al., 2004; Fernandez et al., 2018; Thomas et al., 2021).

445 Overall, the evidence presented here confirms that diatoms preserved in ice cores from the Antarctic Peninsula and Ellsworth Land yield robust, regionally consistent records with the potential to deliver novel environmental proxies and a new chronological tool. Further research should be focused on exploring the spatial relation between the diatom record and environmental parameters.

#### **Data availability**

450 Datasets original to this work will be available at the UK Polar Data Center (<https://www.bas.ac.uk/data/uk-pdc/>).

#### **Author contribution**

DT did the initial conceptualization. DT, CA and ET conducted the formal analysis. DT was in charge of the Investigation. DT and CA designed the Methodology. DT prepared the original manuscript. CA and ET contributed to the reviewing and editing of the original manuscript.

#### 455 **Competing interests**

The authors declare that they have no conflict of interest.

#### **Acknowledgements**

We would like to thank Sarah Crowsley, Tom King, Isobel Rowell and Dr Robert Mulvaney for their help while drilling the SHIC and SKBL ice cores included in this work. We would like to thank Shaun Miller, Dr Jack Humby, Dr Diana  
460 Vladimirova and Dr Daniel Emanuelsson from the Ice core Lab, British Antarctic Survey, for their help while cutting the ice and conducting the Continuous Flow Analysis (CFA). We would like to thank Professor Eric Wolff from the Earth Sciences Department, University of Cambridge, for his comments during the final review and editing of this draft. SEM work was partly supported by a Royal Society Research Professorships Enhancement Award (RP\EA\180006). We would like to thank Dr Iris Buisman and Dr Giulio Lampronti from the Microscopy Lab, Earth Sciences Department, University of Cambridge,  
465 for their technical support in the use of the SEM. This research was funded by CONICYT–Becas Chile and Cambridge Trust funding program for PhD studies. Grant number 72180432.



## References

- Allen, C. S., Pike, J., and Pudsey, C. J.: Last glacial–interglacial sea-ice cover in the SW Atlantic and its potential role in global deglaciation, *Quaternary Science Reviews*, 30, 2446–2458, <https://doi.org/10.1016/j.quascirev.2011.04.002>, 2011.
- 470 Allen, C. S., Thomas, E. R., Blagbrough, H., Tetzner, D. R., Warren, R. A., Ludlow, E. C., and Bracegirdle, T. J.: Preliminary Evidence for the Role Played by South Westerly Wind Strength on the Marine Diatom Content of an Antarctic Peninsula Ice Core (1980–2010), 10, 87, <https://doi.org/10.3390/geosciences10030087>, 2020.
- Alvain, S., Moulin, C., Dandonneau, Y., and Loisel, H.: Seasonal distribution and succession of dominant phytoplankton groups in the global ocean: A satellite view, 22, <https://doi.org/10.1029/2007GB003154>, 2008.
- 475 Armand, L. K., Crosta, X., Romero, O., and Pichon, J.-J.: The biogeography of major diatom taxa in Southern Ocean sediments: 1. Sea ice related species, *Palaeogeography, Palaeoclimatology, Palaeoecology*, 223, 93–126, <https://doi.org/10.1016/j.palaeo.2005.02.015>, 2005.
- Arrigo, K. R., Worthen, D., Schnell, A., and Lizotte, M. P.: Primary production in Southern Ocean waters, 103, 15587–15600, <https://doi.org/10.1029/98JC00930>, 1998.
- 480 Arrigo, K. R., Dijken, G. L. van, and Bushinsky, S.: Primary production in the Southern Ocean, 1997–2006, 113, <https://doi.org/10.1029/2007JC004551>, 2008.
- Arrigo, K. R., Lowry, K. E., and van Dijken, G. L.: Annual changes in sea ice and phytoplankton in polynyas of the Amundsen Sea, Antarctica, *Deep Sea Research Part II: Topical Studies in Oceanography*, 71–76, 5–15, <https://doi.org/10.1016/j.dsr2.2012.03.006>, 2012.
- 485 Barrett, P. J.: Resolving views on Antarctic Neogene glacial history – the Sirius debate, 104, 31–53, <https://doi.org/10.1017/S175569101300008X>, 2013.
- Bouchard, G., Gajewski, K., and Hamilton, P. B.: Freshwater diatom biogeography in the Canadian Arctic Archipelago, 31, 1955–1973, <https://doi.org/10.1111/j.1365-2699.2004.01143.x>, 2004.
- Breider, T. J., Mickley, L. J., Jacob, D. J., Wang, Q., Fisher, J. A., Chang, R. Y.-W., and Alexander, B.: Annual distributions and sources of Arctic aerosol components, aerosol optical depth, and aerosol absorption, 119, 4107–4124, <https://doi.org/10.1002/2013JD020996>, 2014.
- 490 Budgeon, A. L., Roberts, D., Gasparon, M., and Adams, N.: Direct evidence of aeolian deposition of marine diatoms to an ice sheet, 24, 527–535, <https://doi.org/10.1017/S0954102012000235>, 2012.
- Burckle, L. H., Gayley, R. I., Ram, M., and Petit, J.-R.: Diatoms in Antarctic ice cores: Some implications for the glacial history of Antarctica, *Geology*, 16, 326–329, [https://doi.org/10.1130/0091-7613\(1988\)016<0326:DIAICS>2.3.CO;2](https://doi.org/10.1130/0091-7613(1988)016<0326:DIAICS>2.3.CO;2), 1988.
- 495 Cefarelli, A. O., Ferrario, M. E., Almandoz, G. O., Atencio, A. G., Akselman, R., and Vernet, M.: Diversity of the diatom genus *Fragilariopsis* in the Argentine Sea and Antarctic waters: morphology, distribution and abundance, *Polar Biol*, 33, 1463–1484, <https://doi.org/10.1007/s00300-010-0794-z>, 2010.



- Chalmers, M. O., Harper, M. A., and Marshall, W. A.: An illustrated catalogue of airborne microbiota from the maritime  
500 Antarctic, British Antarctic Survey, Cambridge, 175 pp., 1996.
- Cipriano, R. J. and Blanchard, D. C.: Bubble and aerosol spectra produced by a laboratory ‘breaking wave,’ 86, 8085–8092,  
<https://doi.org/10.1029/JC086iC09p08085>, 1981.
- Crosta, X., Romero, O., Armand, L. K., and Pichon, J.-J.: The biogeography of major diatom taxa in Southern Ocean  
sediments: 2. Open ocean related species, *Palaeogeography, Palaeoclimatology, Palaeoecology*, 223, 66–92,  
505 <https://doi.org/10.1016/j.palaeo.2005.03.028>, 2005.
- Delmonte, B., Baroni, C., Andersson, P. S., Narcisi, B., Salvatore, M. C., Petit, J. R., Scarchilli, C., Frezzotti, M., Albani, S.,  
and Maggi, V.: Modern and Holocene aeolian dust variability from Talos Dome (Northern Victoria Land) to the interior of  
the Antarctic ice sheet, *Quaternary Science Reviews*, 64, 76–89, <https://doi.org/10.1016/j.quascirev.2012.11.033>, 2013.
- Delmonte, B., Paleari, C. I., Andò, S., Garzanti, E., Andersson, P. S., Petit, J. R., Crosta, X., Narcisi, B., Baroni, C.,  
510 Salvatore, M. C., Baccolo, G., and Maggi, V.: Causes of dust size variability in central East Antarctica (Dome B):  
Atmospheric transport from expanded South American sources during Marine Isotope Stage 2, *Quaternary Science Reviews*,  
168, 55–68, <https://doi.org/10.1016/j.quascirev.2017.05.009>, 2017.
- Farmer, D. M., McNeil, C. L., and Johnson, B. D.: Evidence for the importance of bubbles in increasing air–sea gas flux,  
361, 620–623, <https://doi.org/10.1038/361620a0>, 1993.
- 515 Fernandes, R., Dupont, S., and Lamaud, E.: Investigating the role of deposition on the size distribution of near-surface dust  
flux during erosion events, *Aeolian Research*, 37, 32–43, <https://doi.org/10.1016/j.aeolia.2019.02.002>, 2019.
- Fernandoy, F., Tetzner, D., Meyer, H., Gacitúa, G., Hoffmann, K., Falk, U., Lambert, F., and MacDonell, S.: New insights  
into the use of stable water isotopes at the northern Antarctic Peninsula as a tool for regional climate studies, 12, 1069–1090,  
<https://doi.org/10.5194/tc-12-1069-2018>, 2018.
- 520 Fetterer, F., K. Knowles, W. N. Meier, M. Savoie, and A. K. Windnagel. Sea Ice Index, Version 3. Sea Ice Extent dataset.  
Boulder, Colorado USA. NSIDC: National Snow and Ice Data Center. <https://doi.org/10.7265/N5K072F8>, 2017.
- Frey, M. M., Bales, R. C., and McConnell, J. R.: Climate sensitivity of the century-scale hydrogen peroxide (H<sub>2</sub>O<sub>2</sub>) record  
preserved in 23 ice cores from West Antarctica, 111, <https://doi.org/10.1029/2005JD006816>, 2006.
- Fritz, S. C., Brinson, B. E., Billups, W. E., and Thompson, L. G.: Diatoms at >5000 Meters in the Quelccaya Summit Dome  
525 Glacier, Peru, 47, 369–374, <https://doi.org/10.1657/AAAR0014-075>, 2015.
- Gayley, R. I., Ram, M., and Stoermer, E. F.: Seasonal variations in diatom abundance and provenance in Greenland ice, 35,  
290–292, <https://doi.org/10.3189/S0022143000004664>, 1989.
- Gonzalez, S. and Fortuny, D.: How robust are the temperature trends on the Antarctic Peninsula?, 30, 322–328,  
<https://doi.org/10.1017/S0954102018000251>, 2018.
- 530 Halse, G. R. and Syvertsen, E. E.: Chapter 2 - Marine Diatoms, in: *Identifying Marine Diatoms and Dinoflagellates*, edited  
by: Tomas, C. R., Academic Press, San Diego, 5–385, <https://doi.org/10.1016/B978-012693015-3/50005-X>, 1996.



- Hamm, C. E., Merkel, R., Springer, O., Jurkojc, P., Maier, C., Prechtel, K., and Smetacek, V.: Architecture and material properties of diatom shells provide effective mechanical protection, *421*, 841–843, <https://doi.org/10.1038/nature01416>, 2003.
- 535 Hamsher, S., Kopalová, K., Kocielek, J., Zidarova, R., and Van De Vijver, B.: The genus *Nitzschia* on the South Shetland Islands and James Ross Island, *16*, 79–102, <https://doi.org/10.5507/fot.2015.023>, 2016.
- Harper, M. A. and McKay, R. M.: Diatoms as markers of atmospheric transport, in: *The Diatoms: Applications for the Environmental and Earth Sciences*, edited by: Stoermer, E. F. and Smol, J. P., Cambridge University Press, Cambridge, 552–559, <https://doi.org/10.1017/CBO9780511763175.032>, 2010.
- 540 Hasle, G. R. and Syvertsen, E. E.: Chapter 2 - Marine Diatoms, in: *Identifying Marine Phytoplankton*, edited by: Tomas, C. R., Academic Press, San Diego, 5–385, <https://doi.org/10.1016/B978-012693018-4/50004-5>, 1997.
- Hausmann, S., Larocque-Tobler, I., Richard, P. J. H., Pienitz, R., St-Onge, G., and Fye, F.: Diatom-inferred wind activity at Lac du Sommet, southern Québec, Canada: A multiproxy paleoclimate reconstruction based on diatoms, chironomids and pollen for the past 9500 years, *The Holocene*, *21*, 925–938, <https://doi.org/10.1177/0959683611400199>, 2011.
- 545 Hazel, J. E. and Stewart, A. L.: Are the Near-Antarctic Easterly Winds Weakening in Response to Enhancement of the Southern Annular Mode?, *32*, 1895–1918, <https://doi.org/10.1175/JCLI-D-18-0402.1>, 2019.
- Kellogg, D. E. and Kellogg, T. B.: Diatoms in South Pole ice: Implications for eolian contamination of Sirius Group deposits, *Geology*, *24*, 115–118, [https://doi.org/10.1130/0091-7613\(1996\)024<0115:DISPII>2.3.CO;2](https://doi.org/10.1130/0091-7613(1996)024<0115:DISPII>2.3.CO;2), 1996.
- Kellogg, D. E. and Kellogg, T. B.: Frozen in Time., in: *Life in Ancient Ice*, edited by: Castello, J. D. and Rogers, S. O., Princeton University Press, 69–93, 2005.
- 550 Koffman, B. G., Kreutz, K. J., Breton, D. J., Kane, E. J., Winski, D. A., Birkel, S. D., Kurbatov, A. V., and Handley, M. J.: Centennial-scale variability of the Southern Hemisphere westerly wind belt in the eastern Pacific over the past two millennia, *10*, 1125–1144, <https://doi.org/10.5194/cp-10-1125-2014>, 2014.
- Lenaerts, J. T. M. and Broeke, M. R. van den: Modeling drifting snow in Antarctica with a regional climate model: 2. Results, *117*, <https://doi.org/10.1029/2010JD015419>, 2012.
- 555 Li, F., Ramaswamy, V., Ginoux, P., Broccoli, A. J., Delworth, T., and Zeng, F.: Toward understanding the dust deposition in Antarctica during the Last Glacial Maximum: Sensitivity studies on plausible causes, *115*, <https://doi.org/10.1029/2010JD014791>, 2010.
- Lichti-Federovich, S. Investigation of diatoms found in surface snow from the Sydkap ice cap, Ellesmere Island, Northwest Territories. *Current Research, Geological Survey of Canada*, 84-01A, 287-301. <https://doi.org/10.4095/119677>, 1984.
- Lizotte, M. P.: The Contributions of Sea Ice Algae to Antarctic Marine Primary Production<sup>1</sup>, *American Zoologist*, *41*, 57–73, <https://doi.org/10.1093/icb/41.1.57>, 2001.
- Lowe, R. L.: Comparative Ultrastructure of the Valves of Some Cyclo<sup>TELL</sup>a Species (bacillariophyceae)<sup>1</sup>, *11*, 415–424, <https://doi.org/10.1111/j.1529-8817.1975.tb02805.x>, 1975.



- 565 Malviya, S., Scalco, E., Audic, S., Vincent, F., Veluchamy, A., Poulain, J., Wincker, P., Iudicone, D., Vargas, C. de, Bittner, L., Zingone, A., and Bowler, C.: Insights into global diatom distribution and diversity in the world's ocean, *PNAS*, 113, E1516–E1525, <https://doi.org/10.1073/pnas.1509523113>, 2016.
- Mayewski, P. A., Maasch, K. A., Dixon, D., Sneed, S. B., Oglesby, R., Korotkikh, E., Potocki, M., Grigholm, B., Kreutz, K., Kurbatov, A. V., Spaulding, N., Stager, J. C., Taylor, K. C., Steig, E. J., White, J., Bertler, N. a. N., Goodwin, I., Simões, J. C., Jaña, R., Kraus, S., and Fastook, J.: West Antarctica's sensitivity to natural and human-forced climate change over the Holocene, 28, 40–48, <https://doi.org/10.1002/jqs.2593>, 2013.
- 570 McKay, R. M., Barrett, P. J., Harper, M. A., and Hannah, M. J.: Atmospheric transport and concentration of diatoms in surficial and glacial sediments of the Allan Hills, Transantarctic Mountains, *Palaeogeography, Palaeoclimatology, Palaeoecology*, 260, 168–183, <https://doi.org/10.1016/j.palaeo.2007.08.014>, 2008.
- 575 Menviel, L., Spence, P., Yu, J., Chamberlain, M. A., Matear, R. J., Meissner, K. J., and England, M. H.: Southern Hemisphere westerlies as a driver of the early deglacial atmospheric CO<sub>2</sub> rise, 9, 2503, <https://doi.org/10.1038/s41467-018-04876-4>, 2018.
- Orr, A., Cresswell, D., Marshall, G. J., Hunt, J. C. R., Sommeria, J., Wang, C. G., and Light, M.: A 'low-level' explanation for the recent large warming trend over the western Antarctic Peninsula involving blocked winds and changes in zonal circulation, 31, <https://doi.org/10.1029/2003GL019160>, 2004.
- 580 Papina, T., Blyakharchuk, T., Eichler, A., Malygina, N., Mitrofanova, E., and Schwikowski, M.: Biological proxies recorded in a Belukha ice core, *Russian Altai*, 9, 2399–2411, <https://doi.org/10.5194/cp-9-2399-2013>, 2013.
- Parkinson, C. L.: A 40-y record reveals gradual Antarctic sea ice increases followed by decreases at rates far exceeding the rates seen in the Arctic, *PNAS*, 116, 14414–14423, <https://doi.org/10.1073/pnas.1906556116>, 2019.
- 585 Parkinson, C. L. and Cavalieri, D. J.: Antarctic sea ice variability and trends, 1979–2010, 6, 871–880, <https://doi.org/10.5194/tc-6-871-2012>, 2012.
- Pasteris, D. R., McConnell, J. R., Das, S. B., Criscitiello, A. S., Evans, M. J., Maselli, O. J., Sigl, M., and Layman, L.: Seasonally resolved ice core records from West Antarctica indicate a sea ice source of sea-salt aerosol and a biomass burning source of ammonium, 119, 9168–9182, <https://doi.org/10.1002/2013JD020720>, 2014.
- 590 Piel, C., Weller, R., Huke, M., and Wagenbach, D.: Atmospheric methane sulfonate and non-sea-salt sulfate records at the European Project for Ice Coring in Antarctica (EPICA) deep-drilling site in Dronning Maud Land, Antarctica, 111, <https://doi.org/10.1029/2005JD006213>, 2006.
- Rigual-Hernández, A. S., Trull, T. W., Bray, S. G., Cortina, A., and Armand, L. K.: Latitudinal and temporal distributions of diatom populations in the pelagic waters of the Subantarctic and Polar Frontal zones of the Southern Ocean and their role in the biological pump, 12, 5309–5337, <https://doi.org/10.5194/bg-12-5309-2015>, 2015.
- 595 Röthlisberger, R., Hutterli, M. A., Sommer, S., Wolff, E. W., and Mulvaney, R.: Factors controlling nitrate in ice cores: Evidence from the Dome C deep ice core, 105, 20565–20572, <https://doi.org/10.1029/2000JD900264>, 2000.



- Rousseaux, C. S. and Gregg, W. W.: Interannual Variation in Phytoplankton Primary Production at A Global Scale, 6, 1–19, <https://doi.org/10.3390/rs6010001>, 2014.
- 600 Simoes, J., Ferron, F., Bernardo, R., Aristarain, A., Stiévenard, M., Pourchet, M., and Delmas, R.: Ice core study from King George Island, South Shetlands, Antarctica, *Pesquisa Antártica Brasileira*, 4, 9–23, 2004.
- Smith, W. O. and Comiso, J. C.: Influence of sea ice on primary production in the Southern Ocean: A satellite perspective, 113, <https://doi.org/10.1029/2007JC004251>, 2008.
- Smol, J. P. and Stoermer, E. F. (Eds.): *The Diatoms: Applications for the Environmental and Earth Sciences*, 2nd ed.,  
605 Cambridge University Press, Cambridge, <https://doi.org/10.1017/CBO9780511763175>, 2010.
- Soppa, M. A., Völker, C., and Bracher, A.: Diatom Phenology in the Southern Ocean: Mean Patterns, Trends and the Role of Climate Oscillations, 8, 420, <https://doi.org/10.3390/rs8050420>, 2016.
- Spaulding, S. A., Van de Vijver, B., Hodgson, D. A., McKnight, D. M., Verleyen, E., and Stanish, L.: Diatoms as indicators of environmental change in Antarctic and subantarctic freshwaters, in: *The Diatoms: Applications for the Environmental and*  
610 *Earth Sciences*, edited by: Stoermer, E. F. and Smol, J. P., Cambridge University Press, Cambridge, 267–284, <https://doi.org/10.1017/CBO9780511763175.015>, 2010.
- Stammerjohn, S., Massom, R., Rind, D., and Martinson, D.: Regions of rapid sea ice change: An inter-hemispheric seasonal comparison, 39, <https://doi.org/10.1029/2012GL050874>, 2012.
- Sudarchikova, N., Mikolajewicz, U., Timmreck, C., O'Donnell, D., Schurgers, G., Sein, D., and Zhang, K.: Modelling of  
615 mineral dust for interglacial and glacial climate conditions with a focus on Antarctica, 11, 765–779, <https://doi.org/10.5194/cp-11-765-2015>, 2015.
- Tesson, S. V. M., Skjøth, C. A., Šantl-Temkiv, T., and Löndahl, J.: Airborne Microalgae: Insights, Opportunities, and Challenges, *Appl. Environ. Microbiol.*, 82, 1978–1991, <https://doi.org/10.1128/AEM.03333-15>, 2016.
- Tetzner, D., Thomas, E., and Allen, C.: A Validation of ERA5 Reanalysis Data in the Southern Antarctic Peninsula—  
620 Ellsworth Land Region, and Its Implications for Ice Core Studies, 9, 289, <https://doi.org/10.3390/geosciences9070289>, 2019.
- Tetzner, D., Thomas, E. R., Allen, C. S., and Wolff, E. W.: A Refined Method to Analyze Insoluble Particulate Matter in Ice Cores, and Its Application to Diatom Sampling in the Antarctic Peninsula, *Front. Earth Sci.*, 9, <https://doi.org/10.3389/feart.2021.617043>, 2021a.
- Tetzner, D. R., Thomas, E. R., Allen, C. S., Piermattei, A. Evidence of recent active volcanism in the Balleny Islands  
625 (Antarctica) from ice core records, *ESSOAr [preprint]*, 10.1002/essoar.10507039.1, 12 May 2021b.
- Thoen, I. U., Simões, J. C., Lindau, F. G. L., Sneed, S. B., Thoen, I. U., Simões, J. C., Lindau, F. G. L., and Sneed, S. B.: Ionic content in an ice core from the West Antarctic Ice Sheet: 1882–2008 A.D., 48, 853–865, <https://doi.org/10.1590/2317-4889201820180037>, 2018.
- Thomas, E. R. and Bracegirdle, T. J.: Improving ice core interpretation using in situ and reanalysis data, 114,  
630 <https://doi.org/10.1029/2009JD012263>, 2009.



- Thomas, E. R. and Bracegirdle, T. J.: Precipitation pathways for five new ice core sites in Ellsworth Land, West Antarctica, *Clim Dyn*, 44, 2067–2078, <https://doi.org/10.1007/s00382-014-2213-6>, 2015.
- Thomas, E. R. and Tetzner, D. R.: The Climate of the Antarctic Peninsula during the Twentieth Century: Evidence from Ice Cores, *IntechOpen*, <https://doi.org/10.5772/intechopen.81507>, 2018.
- 635 Thomas, E. R., Marshall, G. J., and McConnell, J. R.: A doubling in snow accumulation in the western Antarctic Peninsula since 1850, 35, <https://doi.org/10.1029/2007GL032529>, 2008.
- Thomas, E. R., Allen, C. S., Etourneau, J., King, A. C. F., Severi, M., Winton, V. H. L., Mueller, J., Crosta, X., and Peck, V. L.: Antarctic Sea Ice Proxies from Marine and Ice Core Archives Suitable for Reconstructing Sea Ice over the Past 2000 Years, 9, 506, <https://doi.org/10.3390/geosciences9120506>, 2019.
- 640 Thomas, E. R., Gacitúa, G., Pedro, J. B., Faith King, A. C., Markle, B., Potocki, M., and Moser, D. E.: Physical properties of shallow ice cores from Antarctic and sub-Antarctic islands, 15, 1173–1186, <https://doi.org/10.5194/tc-15-1173-2021>, 2021.
- Turner, J., Phillips, T., Hosking, J. S., Marshall, G. J., and Orr, A.: The Amundsen Sea low, 33, 1818–1829, <https://doi.org/10.1002/joc.3558>, 2013.
- Turner, J., Phillips, T., Thamban, M., Rahaman, W., Marshall, G. J., Wille, J. D., Favier, V., Winton, V. H. L., Thomas, E.,
- 645 Wang, Z., Broeke, M. van den, Hosking, J. S., and Lachlan-Cope, T.: The Dominant Role of Extreme Precipitation Events in Antarctic Snowfall Variability, 46, 3502–3511, <https://doi.org/10.1029/2018GL081517>, 2019.
- Van de Vijver, B. and Beyens, L.: Freshwater diatoms from Ile de la Possession (Crozet Archipelago, sub-Antarctica): an ecological assessment, *Polar Biol*, 22, 178–188, <https://doi.org/10.1007/s003000050408>, 1999.
- Wang, L., Lu, H., Liu, J., Gu, Z., Mingram, J., Chu, G., Li, J., Rioual, P., Negendank, J. F. W., Han, J., and Liu, T.: Diatom-
- 650 based inference of variations in the strength of Asian winter monsoon winds between 17,500 and 6000 calendar years B.P., 113, <https://doi.org/10.1029/2008JD010145>, 2008.
- Warnock, J. P. and Scherer, R. P.: Diatom species abundance and morphologically-based dissolution proxies in coastal Southern Ocean assemblages, *Continental Shelf Research*, 102, 1–8, <https://doi.org/10.1016/j.csr.2015.04.012>, 2015.
- Wessem, J. M. van, Reijmer, C. H., Berg, W. J. van de, Broeke, M. R. van den, Cook, A. J., Ulf, L. H. van, and Meijgaard,
- 655 E. van: Temperature and Wind Climate of the Antarctic Peninsula as Simulated by a High-Resolution Regional Atmospheric Climate Model, 28, 7306–7326, <https://doi.org/10.1175/JCLI-D-15-0060.1>, 2015.
- van Wessem, J. M., Ligtenberg, S. R. M., Reijmer, C. H., van de Berg, W. J., van den Broeke, M. R., Barrand, N. E., Thomas, E. R., Turner, J., Wuite, J., Scambos, T. A., and van Meijgaard, E.: The modelled surface mass balance of the Antarctic Peninsula at 5.5 km horizontal resolution, 10, 271–285, <https://doi.org/10.5194/tc-10-271-2016>, 2016.
- 660 Wolff, E. W., Hall, J. S., Mulvaney, R., Pasteur, E. C., Wagenbach, D., and Legrand, M.: Relationship between chemistry of air, fresh snow and firn cores for aerosol species in coastal Antarctica, 103, 11057–11070, <https://doi.org/10.1029/97JD02613>, 1998.
- Young, I. R. and Ribal, A.: Multiplatform evaluation of global trends in wind speed and wave height, 364, 548–552, <https://doi.org/10.1126/science.aav9527>, 2019.



- 665 Yu, L., Zhong, S., and Sun, B.: The Climatology and Trend of Surface Wind Speed over Antarctica and the Southern Ocean and the Implication to Wind Energy Application, 11, 108, <https://doi.org/10.3390/atmos11010108>, 2020.
- Zielinski, U. and Gersonde, R.: Diatom distribution in Southern Ocean surface sediments (Atlantic sector): Implications for paleoenvironmental reconstructions, *Palaeogeography, Palaeoclimatology, Palaeoecology*, 129, 213–250, [https://doi.org/10.1016/S0031-0182\(96\)00130-7](https://doi.org/10.1016/S0031-0182(96)00130-7), 1997.